

Original Article

Gossypol acetic acid induces apoptosis in RAW264.7 cells *via* a caspase-dependent mitochondrial signaling pathway

Sijun Deng¹, Hui Yuan^{1,*}, Jine Yi¹, Yin Lu¹, Qiang Wei¹, Chengzhi Guo², Jing Wu¹, Liyun Yuan^{1,*}, Zuping He^{2,3}

¹College of Veterinary Medicine, Hunan Agricultural University, Changsha 410128, China

²Clinical Stem Cell Research Center, Renji Hospital, Shanghai Jiao Tong University School of Medicine, Shanghai 200127, China

³State Key Laboratory of Oncogenes and Related Genes, Shanghai Cancer Institute, Renji Hospital, Shanghai Jiao Tong University School of Medicine, Shanghai 200032, China

To investigate the effects of gossypol acetic acid (GA) on proliferation and apoptosis of the macrophage cell line RAW264.7 and further understand the possible underlying mechanism responsible for GA-induced cell apoptosis, RAW264.7 cells were treated with GA (25~35 $\mu\text{mol/L}$) for 24 h and the cytotoxicity was determined by MTT assay, while apoptotic cells were identified by TUNEL assay, acridine orange/ethidium bromide staining and flow cytometry. Moreover, mitochondrial membrane potential ($\Delta\Psi_m$) with Rhodamine 123 and reactive oxygen species (ROS) with DCFH-DA were analyzed by fluorescence spectrofluorometry. In addition, the expression of caspase-3 and caspase-9 was assessed by Western Blot assay. Finally, the GA-induced cell apoptosis was evaluated by flow cytometry in the present of caspase inhibitors Z-VAD-FMK and Ac-LEHD-FMK, respectively. GA significantly inhibited the proliferation of RAW264.7 cells in a dose-dependent manner, and caused obvious cell apoptosis and a loss of $\Delta\Psi_m$ in RAW264.7 cells. Moreover, the ROS production in cells was elevated, and the levels of activated caspase-3 and caspase-9 were up-regulated in a dose-dependent manner. Notably, GA-induced cell apoptosis was markedly inhibited by caspase inhibitors. These results suggest that GA-induced RAW264.7 cell apoptosis may be mediated *via* a caspase-dependent mitochondrial signaling pathway.

Keywords: apoptosis, gossypol acetic acid, mitochondrial signaling pathway

Introduction

Gossypol is a yellow phenolic compound with wide

physiological activities that is isolated from the seed of cotton plants [29]. Gossypol has two optical isomers, dextro and levorotation gossypol, with levorotation gossypol being the main active component. Gossypol can also be divided into a free form and combined form. Free gossypol exerts toxic effects *via* its active aldehyde and hydroxyl groups [5]. Gossypol acetic acid (GA) is a medicinal form of gossypol that is more stable to light and heat than gossypol [23]. Gossypol reportedly has various biological actions, including antitumor and anti-parasitic activities, as well as antiviral activity (*e.g.* anti-herpes and anti-HIV) [20]. Gossypol was first investigated as an antifertility agent in the 1960s [8], and has been shown to provoke infertility by suppressing spermatogenesis arrest [4] in males and inhibiting the secretion of progesterone in females [35]. However, there are far fewer reports about its effects on anti-inflammatory and immune function. Therefore, the broad effects of gossypol have received increasing attention in recent years. It has been reported that the anti-inflammatory activity of gossypol could be due to exhausting neutrophils and preventing vasodilatation, which induces inhibition of leukocyte extravasation [12]. Gossypol also suppresses leukemic cell differentiation in response to tumor-promoting phorboids [10] and decreases the expressions of interleukin 2 (IL-2) and interferon γ (IFN- γ) [11]. Mice humoral immune response can also be inhibited by GA, and the immune system is sensitive to GA [8]. Additionally, gossypol prolongs skin allograft survival in mice without affecting the bone marrow function [13]. Therefore, gossypol has been suggested as a potential immunosuppressive agent. Apart from the aforementioned bio-functions, gossypol can readily induce apoptosis in tumor or normal cells, and the existence of distinct

*Corresponding authors: Tel: +86-150-84800501; Fax: +86-731-84673719; E-mail: dykeyan3618@163.com, yuanhui7269@yahoo.com.cn

mechanisms and pathways is involved in gossypol-induced cell apoptosis in different types of cells. For example, gossypol inhibits Bcl-2/Bcl-X_L mediated anti-apoptotic function in mitochondria [21], and the anti-tumor effects of gossypol are mediated *via* ROS-dependent mitochondrial apoptosis in colorectal carcinoma [16]. In human PC-3 prostate cancer cells, gossypol induces apoptosis by regulating both caspase-dependent and -independent cell death pathways [33]. However, the effects of GA-induced apoptosis in the mouse macrophage cell line, RAW264.7, and its downstream effectors have not been reported to date.

To the best of our knowledge, macrophages are one of the most important immune cells in the somatic body, and exert a crucial function in presenting antigens and phagocytosis, resulting in immune response [15]. Thus, macrophages play an important role in the initiation of adaptive immune responses [37]. Macrophages modulate many physiological and immunological functions and are susceptible targets for environmental oxidants [13]. The RAW264.7 cell line was isolated from ascites of BALB/c mice, which is a good model for anti-inflammatory and immunomodulatory studies [18]. Therefore, the present study was conducted to investigate the effects of GA at different concentrations on cell proliferation, apoptosis, mitochondrial transmembrane potential, and ROS production in the mouse macrophage cell line, RAW264.7, and to identify possible signaling pathways responsible for the cytotoxicity of GA in RAW264.7 cells.

Materials and Methods

Reagents

Gossypol acetic acid (GA) was obtained from the College of Light Industry, Zhejiang, China. Dimethyl sulfoxide (DMSO) and an MTT kit were purchased from Sigma-Aldrich (USA). DMEM medium and fetal bovine serum (FBS) were obtained from Gibco (Goitrogen, USA). RIPA lysis buffer, PMSF, caspase inhibitor Z-VAD-FMK, DCFH-DA and Cy3-labeled goat anti-rabbit IgG were acquired from the Beyond Institute of Biotechnology (China). Caspase-9 inhibitor Ac-LEHD-FMK, Rhodamine 123, an ECL detection kit, a TUNEL kit, an acridine orange/stichidium bromide (AO/EB) staining kit and an Anne V-FITC apoptosis detection kit were purchased from Nanjing Kerogen Biotech (China). Antibodies to caspase-3, caspase-9 and β -actin were obtained from Zhongshan Goldenbridge Biotech (China).

Macrophage culture

The mouse macrophage cell line, RAW264.7, was purchased from the Xiang Ya Cell Bank (China). The cell line was cultured and maintained with DMEM medium supplemented with 10% FBS, 1% L-glutamine, 1% penicillin and streptomycin at 37°C in a humidified

incubator with 5% CO₂.

Cell treatment and proliferation by MTT assay

RAW264.7 cells were cultured in the medium as described above in 96-well plates at a density of 1×10^5 cells per well. After culture for 24 h, the cells were treated for 24 h with GA at concentrations ranging from 15 to 40 $\mu\text{mol/L}$, while cells incubated in fresh medium were used as a control. The cell viability was then determined by MTT assay. Briefly, MTT was added to cultures at a final concentration of 5 mg/mL and the samples were incubated for 4 h at 37°C. After gentle removal of the medium, 150 μL DMSO was added to each well to dissolve the formazan product. The absorbance was then measured on a micro-plate reader (AT-858 China) at a wavelength of 490 nm. Cell viability was represented as the relative formazan formation in GA-treated samples compared to a control after correction for background absorbance. The percentage of proliferation inhibition was determined as: % inhibition rate = $[1 - (\text{average absorbance for treated group} / \text{average absorbance for control group})] \times 100$. The IC₅₀ values were obtained from four independent experiments and the assay was repeated four times.

Determination of apoptosis

Apoptosis and necrosis are two completely different cell phenomena. To explore the toxicity of GA, we used the following three methods to detect GA-induced RAW264.7 cell apoptosis.

TUNEL assays

TUNEL detects apoptosis *via* a free 3'-hydroxyl termini on DNA, which is generated in apoptotic cells through cleavage of double-stranded DNA by activated DNA enzymes. Exposed 3'-OH is catalyzed by terminal deoxynucleotidyl transferase enzyme to be linked with digoxigenin-labeled dUTP, then incubated with biotin-labeled anti-digoxigenin antibody and subsequently colored by DAB to enable identification of apoptotic cells under an optical microscope. After RAW264.7 cells were treated with 0, 25, 30 and 35 $\mu\text{mol/L}$ GA for 24 h and fixed with 4% paraformaldehyde for 45 min, a TUNEL assay was conducted according to the manufacturer's instructions. The sections were then observed under a microscope (Olympus, Japan).

AO/EB staining

RAW264.7 cells treated as previously described were harvested and washed three times with PBS, after which 100 μL of cell suspension (about 1×10^6 cells/mL) was incubated with 4 μL of AO/EB solution (1 : 1 v/v). The samples were then shaken gently and 10 μL of sample were placed on a slide with a glass cover slip and examined under a fluorescence microscope (Olympus, Japan).

Annexin-V-FITC/PI detection

The RAW264.7 cells exposed to various concentrations of GA for 24 hours were collected and washed in PBS. The apoptosis rate was then detected by flow cytometry. Briefly, following treatment with different concentrations of GA, cells (1×10^4 cells from each group) were harvested and re-suspended in 1 mL loading buffer, and Annexin V-FITC and PI were added. The mixtures were then held in the dark at room temperature for 10 min, after which they were evaluated by flow cytometry (BD FACscalibur; BD Biosciences, USA) within 1 h.

Measurement of mitochondrial membrane potential ($\Delta\Psi_m$)

The mitochondrial membrane potential was measured in RAW264.7 cells that had been treated with various concentrations of GA for 24 h as described previously [36]. Briefly, cells from different groups were incubated with rhodamine123 (Rh123) at a final concentration of 10 $\mu\text{g}/\text{mL}$ for 30 min in the dark, washed with PBS twice and then centrifuged at $500 \times g$ for 10 min. Finally, absorbance was determined using a spectrofluorometer (F-4500; Hitachi, Japan) at an excitation wavelength of 505 nm and an emission wavelength of 534 nm.

ROS level

ROS levels were monitored using a DCFH-DA cell-permeant probe as previously described [7]. Briefly, the cells from different groups were collected and incubated with 10 $\mu\text{mol}/\text{L}$ DCFH-DA at 37°C for 20 min and then washed with serum-free medium to remove the extracellular DCFH-DA. The fluorescence was then determined at 488 nm excitation and 525 nm emission using a spectrofluorometer.

Western blot analysis

To determine changes in caspase-3 and caspase-9 expression in GA-treated RAW264.7 cells, Western blot analysis was performed as previously described [30]. Briefly, the RAW264.7 cells exposed to GA were washed with PBS and lysed in RIPA lysis buffer supplemented with a mixture of protease-inhibitor (1 mmol/L of PMSF). After 30 min of lysis on ice, cell lysates were centrifuged at 4°C at $14,000 \times g$ for 15 min and the supernatants were then subjected to Western blot analysis. The concentration of protein was subsequently measured by a BioRad Bradford assay with BSA as the standard.

For Western blots, 20 μg of cell lysate from each sample were subjected to SDS-PAGE and then transferred to nitrocellulose membranes. Following blocking with 5% nonfat milk in TBS containing 0.1% Tween-20 (TBST) for 1 hour, the membranes were incubated with the primary antibodies (anti-caspase-3, anti-caspase-9 and anti- β -actin antibody) at a dilution of 1 : 200 to 1 : 500 in TBST at 4°C

overnight. After being washed three times with TBST for 10 min each, the membranes were incubated with a goat anti-rabbit IgG-HRP at a dilution of 1 : 2,000 for 1 hour at room temperature and then washed three times with TBST for 10 min each. The blots were subsequently detected using an ECL detection kit (Beyond China) and exposed to X-OMAT BT film (Kodak, USA). Densitometric analyses of protein bands were processed using the Image-Pro Plus 6.0 software.

The effects of Z-VAD-FMK and Ac-LEHD-FMK on apoptosis induced by GA

To further confirm if GA can induce apoptosis in RAW264.7 cells, Z-VAD-FMK, a nonselective caspase inhibitor that can enter the cells and combine with activated caspase to block apoptosis, and Ac-LEHD-FMK, a specific caspase-9 peptide inhibitor, were used to pretreat RAW264.7 cells for 1 h, after which 35 $\mu\text{mol}/\text{L}$ GA was administered into cultures for 24 h. The cells were then collected, washed in PBS, and analyzed using an Annexin V-FITC/PI kit and flow cytometry.

Statistical analysis

All data are presented as the mean \pm SEM and significant differences ($p < 0.05$) and extremely significant differences ($p < 0.01$) among groups were identified by ANOVA and Tukey's post-hoc test using SPSS 12.0.

Results

The effects of GA on proliferation of RAW264.7 cells

As shown in Fig. 1, after treatment with different concentrations of GA, the proliferation of RAW264.7 cells was progressively inhibited by an increase in the concentration of GA, and the 50% inhibition rate of GA (IC_{50}) was 32.9 $\mu\text{mol}/\text{L}$ after 24 h of incubation. These results indicated that GA could remarkably inhibit RAW264.7 proliferation, and that the cytotoxic effect of GA on the RAW264.7 cells was dose-dependent.

GA-induced apoptosis in RAW264.7 cells

We used a TUNEL assay, AO/EB staining and flow cytometry to elucidate the apoptosis of RAW264.7 cells caused by GA. A TUNEL assay revealed that GA induced a remarkable increase in TUNEL-positive cells in RAW264.7 cells (Fig. 2A ~ D) when compared with the control group. Interestingly, with an increase of GA concentration, the apoptotic RAW264.7 cells increased significantly, while the number of live cells decreased dramatically.

In the AO/EB staining assay, normal cells stained with green fluorescence and necrotic cells with increased cell size, unclear cell profiles or cell structure disruptions were stained with orange-red fluorescence. Apoptotic cells

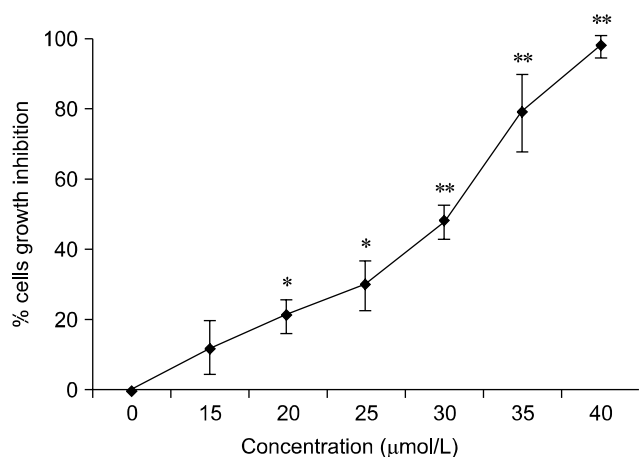


Fig. 1. Effects of GA at different concentrations on the proliferation of RAW264.7 cells measured by MTT assay. Cells were incubated in the absence or presence of GA at different concentrations for 24 h. MTT assay was used to measure the absorbance of RAW264.7 cells at 490 nm. The relative cell growth inhibition was determined as described in the methods. The results shown are one representative of four independent experiments. Compared to the control group, * indicates significant difference ($p < 0.05$), ** indicates extremely significant difference ($p < 0.01$).

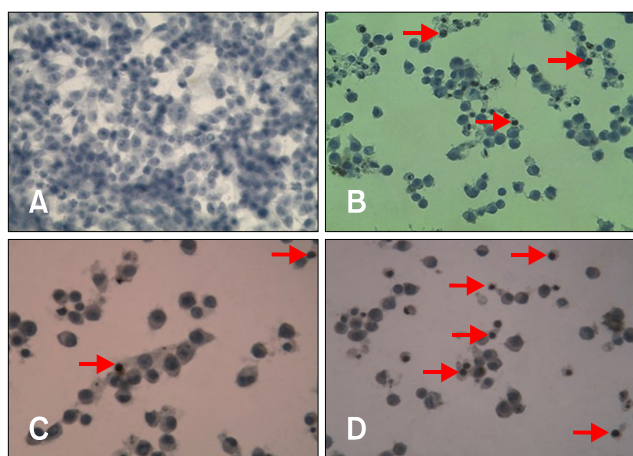


Fig. 2. (A~D) TUNEL assay showing apoptosis of RAW264.7 cells treated with or without GA. Red arrows point to apoptotic cells. (A) Control (normal cells). (B) 25 μmol/L GA-treated cells. (C) 30 μmol/L GA-treated cells. (D) 35 μmol/L GA treated cells. A and B: $\times 200$, C and D: $\times 400$.

showed irregular shape, nuclear margination and condensation. As the GA concentration increased, the number of normal cells decreased significantly, while the appearance of apoptotic cells increased. Additionally, a large number of necrotic cells appeared in the high dose group (Fig. 3A~D).

To quantify the apoptosis rate, cells treated with GA for 24 h were detected by flow cytometry. As shown in Fig. 4, the percentages of apoptotic cells were 30.3%, 63.5% and

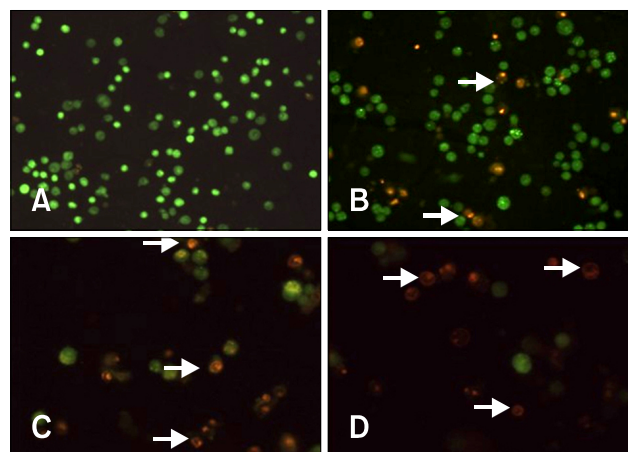


Fig. 3. (A~D) Apoptosis of RAW264.7 cells stained with AO/EB. Red arrows indicate necrotic and apoptotic cells. (A) Control (normal cell). (B) 25 μmol/L GA. (C) 30 μmol/L GA. (D) 35 μmol/L GA. A and B: $\times 100$, C and D: $\times 200$.

79.4%, respectively. These values were dose-dependent and significantly higher than that of the control (4.7%), suggesting that GA induced the apoptosis of RAW264.7 cells in a dose-dependent manner. No obvious differences in the percentages of necrotic RAW264.7 cells treated with or without GA were observed (range = 2.9% to 6.3%). The tendency of apoptotic percentages was consistent with the former results.

Assessment of $\Delta\Psi_m$ in RAW264.7 cells

As a fluorescent indicator of mitochondrial membrane potential ($\Delta\Psi_m$), Rh123 gathers in mitochondria when $\Delta\Psi_m$ increases, while this gathering decreases with decreased $\Delta\Psi_m$, which is accompanied by decreased fluorescence. As shown in Fig. 5, the Rh123 fluorescence intensity of RAW264.7 cells treated with GA decreased significantly in a dose-dependent manner compared to the control, indicating that GA could cause a loss of $\Delta\Psi_m$ in RAW264.7 cells.

GA promoted intracellular ROS level in RAW264.7 cells

Oxidative stress is involved in the toxicities of GA; therefore, we monitored the oxidative stress of RAW264.7 cells exposed to GA. To accomplish this, fluorescent analysis with DCFH-DA was performed to quantify intracellular levels of ROS. As shown in Fig. 6, the DCFH-DA fluorescence of cells increased significantly with increased GA concentrations, suggesting that GA could induce ROS accumulation in RAW264.7 cells.

GA-induced apoptosis is caspase-dependent

To determine whether apoptosis induced by GA was a caspase-dependent mitochondrial signaling pathway, we

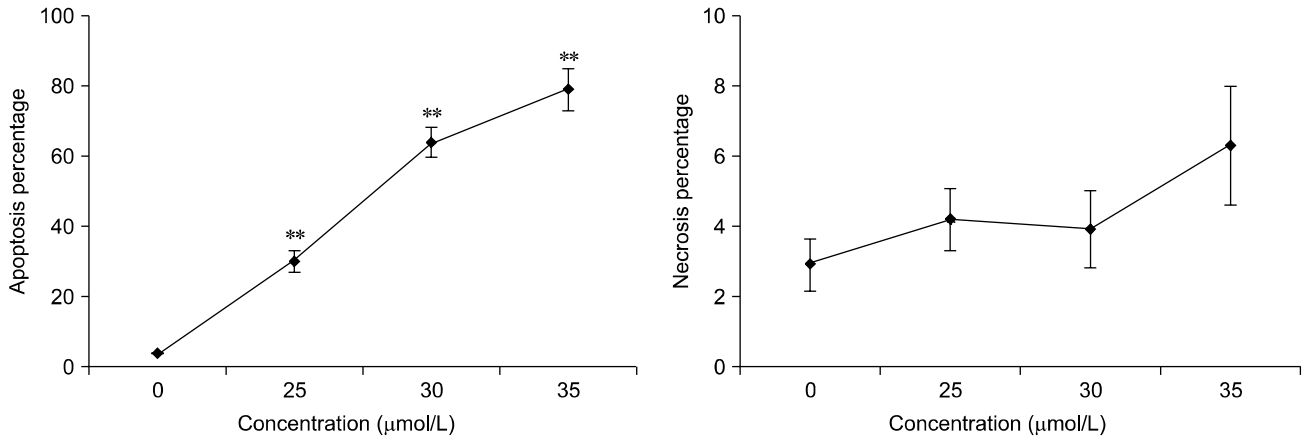


Fig. 4. Flow cytometry showed the apoptosis percentage and necrosis percentage in RAW264.7 cells by GA. Compared to the control group, ** indicates extremely significant difference ($p < 0.01$).

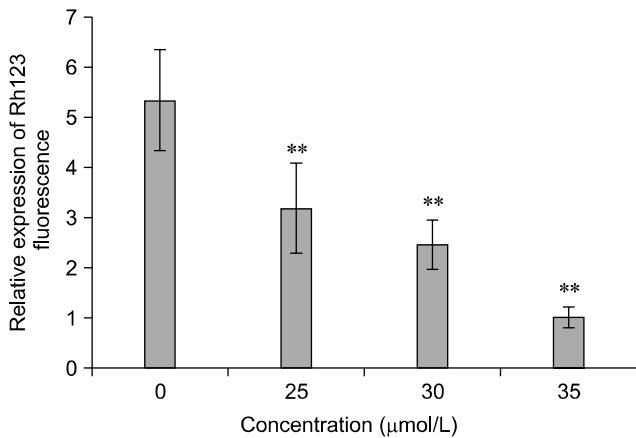


Fig. 5. Changes in mitochondrial transmembrane potential ($\Delta\Psi_m$) in RAW264.7 cells with or without GA treatment as determined by spectrofluorometry. RAW264.7 cells were treated with various concentration of GA for 24 h, after which the Rh123 fluorescence was measured by a spectrofluorometer with an excitation wavelength of 505 nm and an emission wavelength of 534 nm. The expression of Rh123 fluorescence in 35 μmol/L GA treated RAW264.7 cells was designated as 1 and used to calculate the relative expression of Rh123 fluorescence in other groups. The results shown are one representative of three independent experiments. Compared to the control group, ** indicates extremely significant difference ($p < 0.01$).

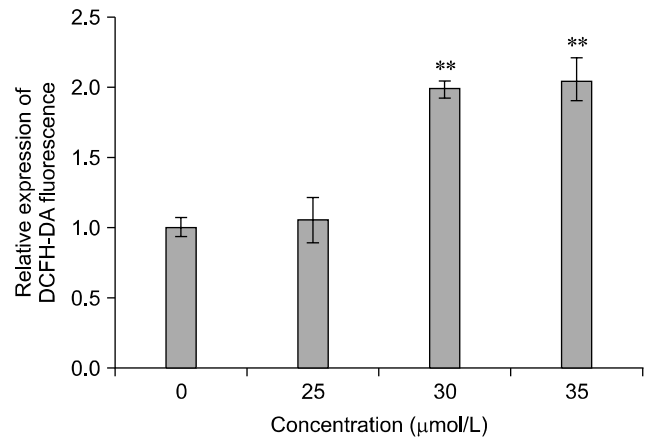


Fig. 6. Levels of ROS in RAW264.7 cells with or without GA treatment as determined by spectrofluorometry. DCFH-DA fluorescence of the cells following GA treatment was measured by a spectrofluorometer with an excitation wavelength of 488 nm and an emission wavelength of 525 nm. The expression of DCFH-DA fluorescence in the control group was designated as 1 and used to calculate the relative expression of DCFH-DA fluorescence in other groups. Compared to the control group, ** indicates extremely significant difference ($p < 0.01$).

examined the effects of the activation of caspase-9 and caspase-3 by Western blot analysis. As shown in Fig. 7, the expression of active-caspase-9 and active-caspase-3 increased in RAW264.7 cells treated with increasing concentrations of GA. In addition, the expression of caspase-9 in cells treated with 35 μmol/L GA was significantly higher than in control cells. To further substantiate the role of caspase-9 in GA-induced apoptosis, cells were pretreated for 1 h with the aforementioned inhibitors prior to 35 μmol/L GA

treatment for 24 h, after which cell apoptosis was determined by flow cytometry. As shown in Fig. 8A~D, the pan-inhibitor and caspase-9 inhibitor significantly decreased GA-induced cell apoptosis from 83% to 74.2% and 64.2%, respectively, while the percentages of living cells were markedly increased from 9.5% to 17.0% and 31.9%, respectively. These results further suggest that GA caused apoptosis in RAW264.7 cells via the caspase-dependent mitochondrial pathway. However, caspase inhibitors cannot completely block GA-induced apoptosis; therefore, there may also be a caspase-independent pathway involved in the GA-induced apoptotic process.

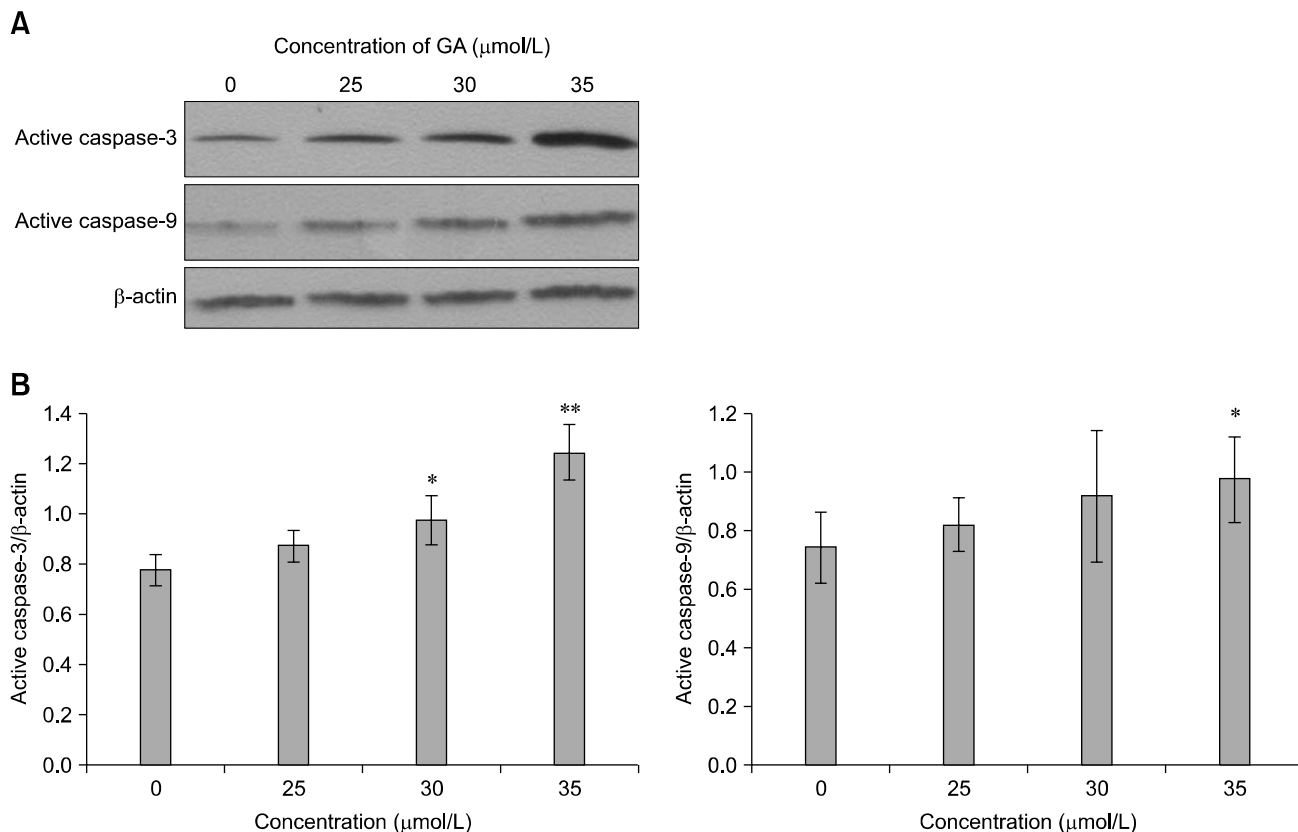


Fig. 7. Expressions of caspase-3 and caspase-9 in RAW264.7 cells without or with GA treatment. (A) Western blots showed the expression of active caspase-3 and active caspase-9 in RAW264.7 cells after GA treatment. β-actin was used as a control for protein loading. (B) Analysis of the intensities of active caspase-3 and active caspase-9 bands (normalized with respect to the intensities of β-actin on the same blots). Compared to the control group, * indicates a significant difference ($p < 0.05$). ** indicates an extremely significant difference ($p < 0.01$).

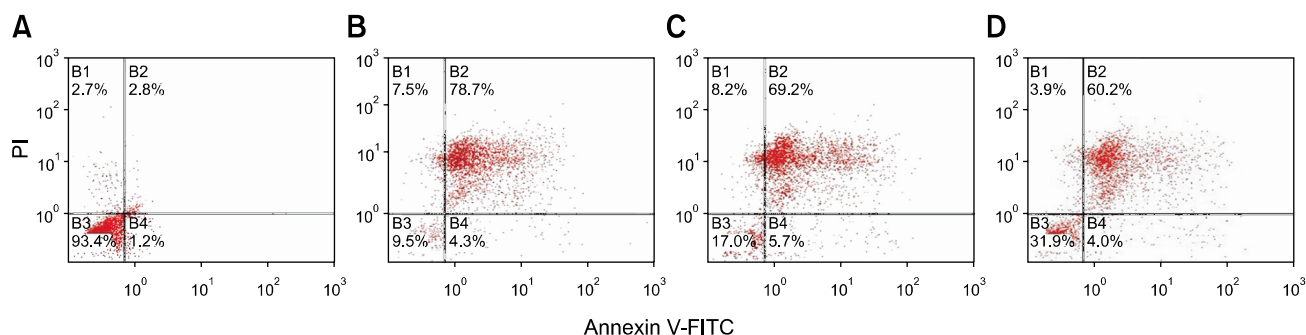


Fig. 8. Flow cytometry analysis of the effects of Z-VAD-FMK and Ac-LEHD-FMK on apoptosis of RAW264.7 cells induced by GA. (A) Control (untreated). (B) Treated with 35 μmol/L GA. (C) Pretreated with 10 μmol/L Z-VAD-FMK and then treated with 35 μmol/L GA. (D) Pretreated with 20 μmol/L Ac-LEHD-FMK and then treated with 35 μmol/L GA.

Discussion

Macrophages are derived from blood monocytes, which are indispensable leukocytes in the body's defense system. These monocytes can differentiate into peritoneal macrophages after migration into ascites [15]. Macrophages can be stimulated by inflammation or

various cytokines, after which they develop into activated macrophages that have greater phagocytic activity and secretion of various active substances, such as increased secretion of inflammatory mediators IL-1 and TNF-α, than other macrophages [20]. Due to the involvement of macrophages in the body's specific and nonspecific immune response, they play an important role in

anti-tumor and anti-infective activities. In the present study, we used the RAW264.7 cell line as a model in inflammatory research to investigate the relationship between GA and cell apoptosis. Our results showed that GA inhibited RAW264.7 cells proliferation in a dose-dependent manner, but that different types of cells had varying sensitivity to GA. The IC_{50} of GA toward RAW264.7 cells was 32.9 $\mu\text{mol/L}$. However, in other studies, the IC_{50} of GA toward the human nasopharyngeal carcinoma cell line CNE2 was 45.24 $\mu\text{mol/L}$ [17], which was similar to the IC_{50} toward the prostate cancer cell lines PC-3 (32.1 $\mu\text{mol/mL}$) and DU-145 at 72 h (31.7 $\mu\text{mol/L}$) [34]. Therefore, the results of the present study indicate a relatively high sensitivity of mouse macrophages to GA. Apoptosis is the process of programmed cell death that may occur in multicellular organisms [14], which is a normal physiological mechanism of maintaining body steady-state. Apoptosis is characterized by a series of morphological changes including cytosol shrinkage, chromatin condensation, nuclei fragmentation and the formation of apoptotic bodies [9]. In RAW264.7 cells exposed to GA, morphological changes could be observed by TUNEL assay. Moreover, flow cytometry and Annexin V-FITC/PI staining revealed that GA caused obvious apoptosis of RAW264.7 cells in a dose-dependent manner. These results were consistent with the results observed for other cell types, including luteal cells in sow [19] and human lymphocytes [32]. Several reports have postulated different mechanisms to explain the cytotoxic effects of GA, *e.g.*, inhibition of several enzymes (protein kinase C, lactate dehydrogenase, adenylate cyclase, acrosin) [25], disruption of cell-to-cell communication at the level of gap junctions [31] and damage to the cellular ultrastructure, with mitochondria being the main target [24].

In mammals, the change in mitochondrial membrane permeability is the first step of the mitochondrial apoptotic pathway, which could lead to loss of $\Delta\Psi_m$, uncoupling of oxidative phosphorylation, increased generation of ROS, depletion of ATP and release of mitochondrial contents (cytochrome C) to the cytoplasm, resulting in apoptosis [28]. ROS is a normal metabolic product of somatic cells and the mitochondria is one of the major organelles for ROS production in cells [22]. ROS functions as redox messengers in intracellular signaling and regulation at low physiological levels, while excess ROS could lead to apoptosis and necrosis [26]. ROS can cause short-term hyperpolarization of the mitochondrial membrane, which leads to further loss of $\Delta\Psi_m$. Therefore, in addition to the role of mitochondria as a source of ROS, it can also be damaged by ROS [30]. Gossypol has been reported to be an uncoupler of oxidative phosphorylation in mitochondria and to disturb mitochondrial oxidative respiration [2]. Thus, gossypol could cause progressive swelling and vacuolization of mitochondria, degradation and

disappearance of mitochondrial cristae, and derangement of the mitochondrial sheath [24]. In this study, we found that GA caused the loss of $\Delta\Psi_m$ in a dose-dependent manner, and that even low concentrations of GA (25 $\mu\text{mol/L}$) caused a dramatic decrease of $\Delta\Psi_m$. In our experiments, we found that a large amount of ROS was produced when RAW264.7 cells were stimulated using 35 $\mu\text{mol/L}$ of GA. It has been reported that ROS is a hypothesized trigger of endogenous apoptotic cascade reactions by interactions with the proteins of the mitochondrial permeability transition complex [1], and ROS also plays direct or indirect roles in the activation of caspases [26]. Therefore, these data suggested that the damage to mitochondria in macrophages is caused by GA, and that the excessive ROS induced by GA may be responsible for cell apoptosis of RAW264.7 cells.

The occurrence of apoptosis generally arises from various apoptotic pathways in different environments, such as cells and stimulations. Apoptosis is mainly mediated through at least three major pathways regulated by the (1) mitochondrial apoptotic pathway, (2) death receptor pathway, and (3) endoplasmic reticulum pathway. These three mechanisms interact with each other's intracellular network systems [3]. Comparatively, the mitochondrial pathway is the most important intracellular apoptosis signaling cascade, and this main mechanism is accompanied by $\Delta\Psi_m$ depolarization followed by cytochrome C release from the mitochondria into the cytosol, where cytochrome C binds with Apaf-1 to further activate caspase-9, which in turn activates caspase-3 [27]. Therefore, caspases are central mediators of apoptosis, and caspase-3 is a prevalent caspase that is ultimately responsible for the majority of apoptotic processes [6]. In the present study, when RAW264.7 cells were subjected to treatment with various concentrations of GA, activated caspase-3 and caspase-9 in cells increased markedly in a dose-dependent manner, and the expression of caspase-3 and caspase-9 in treated groups was higher than in the control groups. Notably, both pan-caspase inhibitor Z-VAD-FMK and caspase-9 inhibitor Ac-LEHD-FMK decreased the apoptosis induced by GA. These data in combination with the expression of activated caspases indicate that GA-induced apoptosis may be mediated *via* the caspase-dependent pathway in RAW264.7 cells, but that caspase inhibitors cannot completely block the GA-induced apoptosis. Therefore, there may be other synergistic pathways acting together in this process, which is consistent with the results of previous studies [33].

In summary, the results of the present study demonstrate that GA inhibited proliferation and induced apoptosis in RAW264.7 cells, and that GA-induced apoptosis of RAW264.7 cells was mediated through a caspase-dependent mitochondrial signaling pathway. In addition, GA caused the loss of $\Delta\Psi_m$ of RAW264.7 cells,

but increased ROS levels of the cells. Our study highlights the cytotoxicity of GA toward macrophages and may provide evidence useful for future investigations of the immunomodulatory effects of GA.

Acknowledgments

Our research was supported from National Natural Science Foundation of China (Grant No.31201964), Research Fund for the Doctoral Program of Higher Education of China (Grant No.20124320120011), Department of Education of Hunan Province, China (Key project No.12A066), Hunan Provincial Key Laboratory of Crop Germplasm Innovation and Utilization of China (Opening Science Fund No. 12KFXM08).

References

1. **Borutaite V.** Mitochondria as decision-makers in cell death. *Environ Mol Mutagen* 2010, **51**, 406-416.
2. **Cheng W, Li Y, Yang D, Zhao Y.** Effect of gossypol acetate on proliferation and apoptosis in Raji lymphoblastoid cell line. *Zhongguo Yi Xue Ke Xue Yuan Xue Bao* 2009, **31**, 527-532.
3. **Chowdhury I, Tharakan B, Bhat GK.** Current concepts in apoptosis: the physiological suicide program revisited. *Cell Mol Biol Lett* 2006, **11**, 506-525.
4. **Coutinho EM.** Gossypol: a contraceptive for men. *Contraception* 2002, **65**, 259-263.
5. **Dao VT, Gaspard C, Mayer M, Werner GH, Nguyen SN, Michelot RJ.** Synthesis and cytotoxicity of gossypol related compounds. *Eur J Med Chem* 2000, **35**, 805-813.
6. **Denault JB, Salvesen GS.** Apoptotic caspase activation and activity. *Methods Mol Biol* 2008, **414**, 191-220.
7. **Deng S, Pawlak A, Poźniak B, Suszko A, Szczypka M, Yuan H, Obmińska-Mrukowicz B.** Effects of gossypol acetic acid on cellular and humoral immune response in non-immunized and SRBC-immunized mice. *Centr Eur J Immunol* 2012, **37**, 11-19.
8. **Dodou K, Anderson RJ, Small DA, Groundwater PW.** Investigations on gossypol: past and present developments. *Expert Opin Investig Drugs* 2005, **14**, 1419-1434.
9. **Earnshaw WC, Martins LM, Kaufmann SH.** Mammalian caspases: structure, activation, substrates, and functions during apoptosis. *Annu Rev Biochem* 1999, **68**, 383-424.
10. **Hass R, Pfannkuche HJ, Kharhanda S, Gunji H, Meyer G, Hartmann A, Hidaka H, Resch K, Kufe D, Goppelt-Strübe M.** Protein kinase C activation and protooncogene expression in differentiation/retrodifferentiation of human U-937 leukemia cells. *Cell Growth Differ* 1991, **2**, 541-548.
11. **He X, Zeng Y, Xu L, Sun H, Li Z, Di J.** Influences of protein kinase C inhibitors on the expression of IL-2 and IFN- γ by human T-lymphocytes. *Chin J Pathophysiol* 2002, **18**, 522-525.
12. **Hu CY, Jiang CH.** The biological activities and mechanisms of gossypol. *Foreign Medical Sciences (Family Planning/Reproductive Health Fascicle)* 1997, **16**, 68-72.
13. **Huang MM, Shao XX, Xiong ZH, Mao YE, Ouyang YG.** The experimental research of taurine sodium gossypol immunosuppression. *Acta Med Univ Sci Technol Huazhong* 1981, **10**, 77.
14. **Jacobson MD, Weil M, Raff MC.** Programmed cell death in animal development. *Cell* 1997, **88**, 347-354.
15. **Kindt TJ, Osborne BA, Goldsby RA.** *Kuby Immunology*. 6th ed. pp.37-44, W.H. Freeman, New York, 2006.
16. **Ko CH, Shen SC, Yang LY.** Gossypol reduction of tumor growth through ROS-dependent mitochondria pathway in human colorectal carcinoma cells. *Int J Cancer* 2007, **121**, 1670-1679.
17. **Liang L, Wang SM, Hu XG, Cao MM, Zhang JR.** Effects of gossypol acetic acid on CNE2 cells apoptosis. *J Pract Med* 2008, **24**, 1009-1101.
18. **Lin HW, Chang TJ, Yang DJ, Chen YC, Wang M, Chang YY.** Regulation of virus-induced inflammatory response by β -carotene in RAW264.7 cells. *Food Chem* 2012, **134**, 2169-2175.
19. **Long A, Wu J, Yuan L, Yuan H.** Effect of gossypol on proliferation and apoptosis of primary luteal cells in sow. *Chin J Vet Sci* 2009, **29**, 1303-1306.
20. **Lowenstein CJ, Dinerman JL, Snyder SH.** Nitric oxide: a physiologic messenger. *Ann Intern Med* 1994, **120**, 227-237.
21. **Oliver CL, Miranda MB, Shangary S, Land S, Wang S, Johnson DE.** (-)-Gossypol acts directly on the mitochondria to overcome Bcl-2- and Bcl-X_L-mediated apoptosis resistance. *Mol Cancer Ther* 2005, **4**, 23-31.
22. **Orrenius S, Gogvadze V, Zhivotovskiy B.** Mitochondrial oxidative stress: implications for cell death. *Annu Rev Pharmacol Toxicol* 2007, **47**, 143-183.
23. **Prasad MRN, Diczfalusy E.** Gossypol. *Int J Androl* 1982, **5** (Suppl 5), 53-70.
24. **Robinson JM, Tanphaichitr N, Bellvé AR.** Gossypol-induced damage to mitochondria of transformed Sertoli cells. *Am J Pathol* 1986, **125**, 484-492.
25. **Qian SZ, Wang ZG.** Gossypol: a potential antifertility agent for males. *Annu Rev Pharmacol Toxicol* 1984, **24**, 329-360.
26. **Simon HU, Haj-Yehia A, Levi-Schaffer F.** Role of reactive oxygen species (ROS) in apoptosis induction. *Apoptosis* 2000, **5**, 415-418.
27. **Slee EA, Harte MT, Kluck RM, Wolf BB, Casiano CA, Newmeyer DD, Wang HG, Reed JC, Nicholson DW, Alnemri ES, Green DR, Martin SJ.** Ordering the cytochrome c-initiated caspase cascade: hierarchical activation of caspases-2, -3, -6, -7, -8, and -10 in a caspase-9-dependent manner. *J Cell Biol* 1999, **144**, 281-292.
28. **Tiwari BS, Belenghi B, Levine A.** Oxidative stress increased respiration and generation of reactive oxygen species, resulting in ATP depletion, opening of mitochondrial permeability transition, and programmed cell death. *Plant Physiol* 2002, **128**, 1271-1281.
29. **Wang X, Howell CP, Chen F, Yin J, Jiang Y.** Gossypol-A Polyphenolic Compound from Cotton Plant. *Adv Food Nutr Res* 2009, **58**, 215-263.
30. **Wu J, Jing L, Yuan H, Peng S.** T-2 toxin induces apoptosis in ovarian granulosa cells of rats through reactive oxygen species-mediated mitochondrial pathway. *Toxicol Lett* 2011, **202**, 168-177.

31. **Ye YX, Bombick D, Hirst K, Zhang GX, Chang CC, Trosko JE, Akera T.** The modulation of gap junctional communication by gossypol in various mammalian cell lines in vitro. *Fundam Appl Toxicol* 1990, **14**, 817-832.
32. **Yurtcu E, Ergun MA, Menevse A.** Apoptotic effect of gossypol on human lymphocytes. *Cell Bio Int* 2003, **27**, 791-794.
33. **Zhang M, Liu H, Tian Z, Griffith BN, Ji M, Li QQ.** Gossypol induces apoptosis in human PC-3 prostate cancer cells by modulating caspase-dependent and caspase-independent cell death pathways. *Life Sci* 2007, **80**, 767-774.
34. **Zhan WH, Yan G, Shao SP.** Observation of apoptotic effect on human prostate cancer cell PC-3 and DU-145 induced by (–)-gossypol. *Shandong Medicine* 2008, **48**, 86-87.
35. **Zheng YH, Wu ZH, Fang L.** Effect of gossypol acetic acid on hCG-stimulated progesterone production of dissociated rat luteal cells. *Yao Xue Xue Bao* 1991, **26**, 805-808.
36. **Zhu L, Yuan H, Guo C, Lu Y, Deng S, Yang Y, Wei Q, Wen L, He Z.** Zearalenone induces apoptosis and necrosis in porcine granulosa cells via a caspase-3- and caspase-9-dependent mitochondrial signaling pathway. *J Cell Physiol* 2012, **227**, 1814-1820.
37. **Zirk NM, Hashmi SF, Ziegler HK.** The polysaccharide portion of lipopolysaccharide regulates antigen-specific T-cell activation via effects on macrophage-mediated antigen processing. *Infect Immun* 1999, **67**, 319-326.